Investigation of NO_2 and NO interaction with an Fe-ZSM-5 catalyst by transient response methods and chemical trapping techniques

Maria Pia Ruggeri, Tommaso Selleri, Massimo Colombo, Isabella Nova, Enrico Tronconi *

Dipartimento di Energia, Laboratorio di Catalisi e Processi Catalitici, Politecnico di Milano, Via La Masa 34, I-20156 Milan, Italy

Received 6 October 2014
Revised 23 January 2015
Accepted 5 February 2015

This paper is dedicated to the memory of Haldor Topsøe.

1. Introduction

Emissions regulations for compression- and spark-ignited internal combustion engines are becoming more and more stringent worldwide and, in many cases, it is no longer possible to achieve the limits imposed by international legislation by just improving combustion process technology. These considerations have led the automotive industry to promote intensive research work in order to develop effective after-treatment systems able to meet emission standards for all the main classes of pollutants. Nowadays a significant part of this effort is focused on the design and improvement of after-treatment systems for the control of NO_x emissions from diesel engines. In this area both lean NO_x traps (LNT) and NH_3/urea-selective catalytic reduction (NH_3/urea-SCR) have been successfully demonstrated at the commercial scale. In NH_3-SCR converters, excellent deNO_x performance is achieved over metal-promoted zeolite catalysts thanks to their activity in two main reactions, the standard SCR reaction ($NO + O_2 + NH_3$) and the fast SCR reaction ($NO + NO_2 + NH_3$) [1]. In recent years, several studies [1–11] have addressed the SCR catalytic mechanism over state-of-the-art metal-exchanged zeolites, in order to determine the related intermediates and to conclusively identify the rate-determining step for both reactions. Attention has been focused mostly on the fast SCR mechanism, which is more efficient in the reduction of NO_x at low temperatures. In this case it is generally accepted that the rate-determining step at low temperature is associated with the reduction of surface nitrates to nitrites by NO [5,12].

For the standard SCR chemistry, on the other hand, the situation is more complex and still debated. Historically, a simple sequential scheme has been proposed, wherein NO is first oxidized to NO_2 in a slow rate-determining step; then NO_2 rapidly reacts with additional NO according to fast SCR stoichiometry. Recently, however, multiple experimental results showing inconsistencies between NO oxidation to NO_2 and the standard SCR mechanisms on Fe- and Cu-promoted zeolites have been reported in the literature [13–18]. In particular, it has been shown that under many circumstances there is hardly any correlation between the rate of NO oxidation to NO_2 and the rate of the standard SCR reaction [13,18]. Thus, although it is generally agreed that the standard SCR reaction mechanism is initiated at low temperature by the oxidative activation of NO, the nature of the reactive intermediate generated at this step is still a matter of discussion. At least three different types of

* Corresponding author.
E-mail address: enrico.tronconi@polimi.it (E. Tronconi).

intermediate have been proposed: nitrates (formal oxidation state N = +5) [11,19], nitrosonium ions (NO^+, formal oxidation state N = +3) [10], and nitrites (formal oxidation state N = +3) [13]. While in situ FTIR evidence for the formation of both nitrates and NO^+ under SCR reaction conditions has been reported, this is not the case for nitrites. As a matter of fact, nitrites can hardly be detected on zeolites by IR spectroscopic techniques, since their characteristic bands, e.g., at 1260 cm^{-1}, fall into the same absorbance region of the zeolite framework (wavenumbers < 1300 cm^{-1}) [12,20]. Furthermore, nitrites are known to be highly reactive and unstable.

In a preliminary communication, we have recently reported that nitrites formed by NO oxidation at 120 °C over Fe-ZSM-5 can indeed be detected by trapping them on BaO/Al_2O_3 [21]. In this paper we present a new, more extended set of experiments addressing comparatively the interaction of NO_2 and NO with the same Fe-zeolite catalyst in the presence of oxygen. In particular, three different systems are analyzed: (i) an Fe-ZSM-5 commercial catalyst, playing the role of active phase, (ii) a BaO/Al_2O_3 prepared in house, acting as a chemical NO_x trap in view of its well-known capability to store stable nitrites and nitrates [24], and (iii) a mechanical mixture of these two compounds. Depending on the system under study, different experiments are performed, including (i) NO_2 adsorption at 120 °C, followed by a temperature ramp (TPD) to analyze the decomposition of the adspecies stored during the isothermal adsorption phase; (ii) NO_2 adsorption at 120 °C, followed by a temperature ramp while feeding NO (TPSR in NO), in order to probe the reactivity of the adsorbed species with NO; (iii) adsorption of NO + O_2 at 120 °C, followed by TPD; (iv) NO + O_2 adsorption at 120 °C, followed by TPSR in NH_3; and (v) NH_3 adsorption at 120 °C, followed by TPSR in NO + O_2. In addition, ex situ IR spectroscopy is also applied to conclusively identify the intermediates captured onto both the BaO and the Fe-ZSM-5 phases.

The data collected provide new experimental evidence in favor of the hypothesis that the initial activation of NO proceeds at low temperatures via nitrite adspecies, NO_2^-, acting therefore as intermediates in both NO oxidation to NO_2 [22] and NO + NH_3 standard SCR reactions [23]. Moreover, they also show that surface nitrates, obtained by NO_2 disproportionation, are not the primary products of the oxidative activation of NO on Fe-promoted zeolite catalysts.

Finally, we propose a low-temperature mechanism of NO oxidation that is consistent with all the experimental results presented herein.

2. Experimental

Three different systems in powder form are analyzed in the present study: a commercial (Zeolyst) Fe-ZSM-5 catalyst (22 mg, Fe loading = 1% w/w, Si/Al = 12), an in-house prepared BaO/Al_2O_3 working as a NO_x trap (44 mg, Ba content = 16% w/w), and a mechanical mixture of these two compounds (22 mg + 44 mg). The relative amounts of the two components were selected to ensure a large excess of potential Ba storage sites with respect to the Fe sites. All the powders were diluted up to a total weight of 160 mg with cordierite and then loaded into a quartz flow microreactor.

Additional details regarding the experimental setup and the preparation and characterization of the tested samples can be found in [21].

When loaded into the microreactor, each new sample was conditioned once for 6 h at 600 °C in a continuous flow of 10% v/v H_2O and 10% O_2 in He. In addition, prior to each run, the samples were pretreated by feeding 8% v/v O_2 + He at 550 °C continuously for 1 h and then also during the cooling-down transient to the test temperature (typically 120 °C). The pretreatment part has been omitted in the reported results: the data acquisition started ($t = 0$) when the test temperature was reached.

Helium was used as the balance gas in all the microreactor runs. Gases from calibrated NO + He, NO_2 + He, O_2 + He bottled mixtures were dosed using mass flow controllers (Brooks Instruments), while water vapor was added to the feed stream by means of a saturator operated at controlled temperature. NO and O_2 were fed into the reactor via independent lines and mixed just at the reactor inlet in order to prevent formation of any NO_2 upstream of the catalyst bed. The purity of the NO + He mixture was checked by a UV analyzer during preliminary calibrations.

The gas phase experiments consisted of two separate stages involving first an isothermal adsorption, followed by a purge in inert gas (He) at the same temperature; the second stage was a linear temperature ramp up to 550 °C at 15 °C/min with or without the addition of a reagent. In a first set of runs, the adsorption of 500 ppm of NO_2 was performed in the presence of 8% v/v O_2, followed by temperature-programmed desorption (TPD). In this way the nature of the species stored during NO_2 adsorption and their stability were investigated. In a second type of experiment, after the same NO_2 adsorption phase, the reactivity of the stored species with NO was tested in a temperature-programmed surface reaction (TPSR) run. In this phase 500 ppm of NO was fed into the reactor and, once the concentration profiles reached a stationary condition, the temperature was increased at 15 °C/min up to 550 °C. In a third class of experiments, the adsorption of 500 ppm of NO at 120 °C in the presence of 8% v/v O_2 was performed, followed by a TPD phase involving the release of the adspecies possibly trapped on the BaO/Al_2O_3. In a fourth set of experiments, the reactivity of the adspecies stored after 500 ppm NO + 8% v/v O_2 adsorption at 120 °C was tested by feeding 500 ppm of NH_3 (TPSR). Finally, additional gas phase experiments were conducted by adsorbing 500 ppm of NH_3 at 120 °C and observing its reactivity with 500 ppm of NO and 8% v/v O_2 during a TPSR test.

FTIR analysis was performed ex situ, unloading the powders from the microreactor after the isothermal adsorption of either NO_2 or NO + O_2. In particular, for the mechanical mixture, different particle sizes were used for its two components (90 μm for the Fe-ZSM-5 and 115 μm for the BaO/Al_2O_3) to enable their separation by sieving. Furthermore, no cordierite was added for dilution in these cases. The choice of the mesh sizes for the two components was the result of optimization of the sieving process. The separation efficiency of the sieving operation was eventually confirmed by the IR results: in fact, residual Fe-ZSM-5 powders in the BaO/Al_2O_3 samples, if present in significant amounts, would be easily recognized during the IR analysis by the typical T–O–T vibration features of the zeolite below 1000 cm^{-1}, which were not detected, however. Additional details on the ex situ FTIR measurements are provided in [21].

3. Results and discussion

3.1. Catalytic activity in standard SCR

Fig. 1 compares standard SCR steady-state activity runs over Fe-ZSM-5 and over the mechanical mixture of Fe-ZSM-5 and BaO/Al_2O_3. From Fig. 1 it is evident that the Fe-ZSM-5 sample exhibits the typical NH_3 SCR activity of Fe-zeolites [1,5], and that the presence of BaO did not affect the original catalytic performance of Fe-ZSM-5. This preliminary test therefore confirms the feasibility of running reactivity experiments over the mechanical mixture to gain insight into the interactions between NO or NO_2 and the Fe-zeolite catalysts under representative SCR conditions.

It may be worth pointing out also that the good standard SCR activity exhibited by both the Fe-ZSM-5-containing phases in

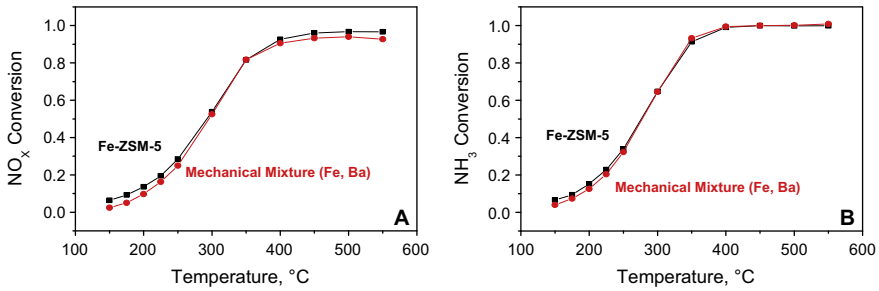

Fig. 1. Reactivity of NH_3–NO–O_2 as a function of temperature: Q = 172 cm^3/min (STP), NH_3 = 500 ppm, NO = 500 ppm, H_2O = 5%, O_2 = 2% on Fe-ZSM-5 (black squares) and on Fe-ZSM-5 + BaO/Al_2O_3 mechanical mixture (red dots) samples: (A) NO_x conversion, (B) NH_3 conversion. (For interpretation of the references to color in this figure legend, the reader is referred to the web version of this article.)

Fig. 1 confirms that the conditioning pretreatment did not significantly alter the structure of the catalyst, which was still fully representative of technical Fe-zeolite SCR catalysts.

3.2. NO_2 adsorption

In the following section the interaction of NO_2 with Fe-ZSM-5, with BaO/Al_2O_3, and with their physical mixture is studied and discussed. In fact, several authors designate NO_2 as an intermediate of primary importance in the standard SCR reaction [14,17,25].

3.2.1. NO_2 adsorption + TPD

Fig. 2A shows results from isothermal NO_2 adsorption at 120 °C on an Fe-ZSM-5 catalyst sample diluted with cordierite. The NO_2 outlet concentration trace exhibits a significant delay, on the order of 60 s, as well as pronounced dynamics, approaching the steady state very slowly. In addition, simultaneous evolution of NO is observed. This is related to the well-known NO_2 disproportionation mechanism [5,26–28] leading to the storage of nitrates [21,27]:

$$2NO_{2,(g)} + O^{2-}_{(ads)} \leftrightarrow NO^{-}_{2,(ads)} + NO^{-}_{3,(ads)}, \quad (R.1)$$

$$NO^{-}_{2,(ads)} + NO_{2,(g)} \leftrightarrow NO_{(g)} + NO^{-}_{3,(ads)}. \quad (R.2)$$

On combining (R.1) and (R.2),

$$3NO_{2,(g)} + O^{2-}_{(ads)} \leftrightarrow 2NO^{-}_{3,(ads)} + NO_{(g)}. \quad (R.3)$$

We can rewrite the mechanism for the storage of nitrates specifically on Fe-ZSM-5 as

$$3NO_{2,(g)} + 2Fe^{3+}(OH^{-}) \leftrightarrow 2Fe^{3+}(NO^{-}_{3}) + NO_{(g)} + H_2O_{(g)} \quad (R.4)$$

The ratio between produced NO and consumed NO_2 is also plotted in Fig. 2A (dashed orange[1] line): a value of approximately 1/3 is obtained, as expected for a fully preoxidized catalyst [27] in which the reoxidation of reduced Fe sites by NO_2 is negligible.

Fig. 2B shows the TPD curves resulting from the decomposition of the species stored on Fe-ZSM-5. The NO_2 concentration trace exhibits a shoulder at 250 °C and a main peak at 300 °C, likely due to the different stabilities of multiple adsorbed nitrates species. The obtained profile is in line with the results found in the literature for the decomposition of ferric nitrates [27]:

$$2Fe^{3+}(NO^{-}_{3}) \rightarrow 2NO_{2,(g)} + 2Fe^{2+} + O_{2,(g)}. \quad (R.5)$$

The time integral of the NO_x trace, obtained by summing the NO and NO_2 concentration profiles at the reactor outlet, provides the overall quantity of nitrates stored, which is 0.0047 $mmol_{NOx}$, corresponding to 12% of the available Fe atoms, in line with literature results [27]. Quantities stored during the adsorption phase differ from the total NO_x desorbed during the TPD by less than 5%. Note that the indicated NO_x storage capacities are presented in absolute terms, i.e., not ratioed to the catalyst load (or to the Fe content), in order to enable a direct comparison with the values measured on the mechanical mixture, for which specific storage capacities are of course meaningless.

An analogous experiment has been performed on the individual BaO/Al_2O_3 sample. Fig. 2C illustrates the isothermal NO_2 adsorption phase. It is possible to appreciate the longer delay (200 s) and the slower dynamics (stationary after 1500 s) of the NO_2 concentration trace, reflecting the much higher NO_x storage capacity of the barium oxide than of the Fe-zeolite, as confirmed by integral calculations (0.0463 $mmol_{NOx}$ vs. 0.0047 $mmol_{NOx}$) and in line with literature results [29]. Indeed, it is well known that barium oxide is able to store nitrates according to the global disproportionation reaction

$$3NO_{2,(g)} + BaO \leftrightarrow Ba(NO_3)_2 + NO_{(g)}. \quad (R.6)$$

The TPD curve for BaO/Al_2O_3 in Fig. 2D shows a single main NO_2 peak at 450 °C. This means that the stored barium nitrates are quite more stable than the corresponding nitrates on Fe-ZSM-5, which are associated with a NO_2 TPD peak centered around 300 °C. Moreover, decomposition of NO_2 to NO and O_2 is evident at high temperatures in this case, according to the reaction [27]

$$NO_{2,(g)} \leftrightarrow NO_{(g)} + \frac{1}{2}O_{2,(g)}. \quad (R.7)$$

In general, the results of NO_2 adsorption on BaO/Al_2O_3 are in agreement with the LNT literature, such as [30,31]. The integral balance of NO_x is closed with an error below 10%. The moles of desorbed NO_x (0.0463 $mmol_{NOx}$, as previously reported) correspond to about 39% of the overall number of available Ba sites, again in agreement with literature data [29].

Finally, Fig. 2E shows the isothermal NO_2 adsorption phase on the mechanical mixture of Fe-ZSM-5 and BaO/Al_2O_3. The observed behavior is quite similar to that noted on BaO/Al_2O_3 alone (Fig. 2C). The NO_x storage capacity, however, is increased in this case and is very close to the sum of the capacities of the two single phases (the difference is less than 3%): thus we can rule out a synergy between the two mixture components during NO_2 adsorption. The moles of adsorbed NO_x (0.0549 $mmol_{NOx}$) correspond to about 43% of the overall number of sites, in agreement with our findings on the BaO/Al_2O_3 phase alone and with LNT literature data [29]. NO_x storage takes place essentially on the BaO/Al_2O_3 phase, with only a limited contribution (on the order of 5%) of the Fe-ZSM-5 sites. The integral balance of NO_x over the whole run (adsorption + TPD) is closed with an error of about 10%.

Interestingly, the situation is different during the TPD phase, displayed in Fig. 2F, where NO_2 is desorbed with a main peak at 350 °C, i.e., at a temperature in between those of the NO_2 peaks

[1] For interpretation of color in Fig. 2, the reader is referred to the web version of this article.

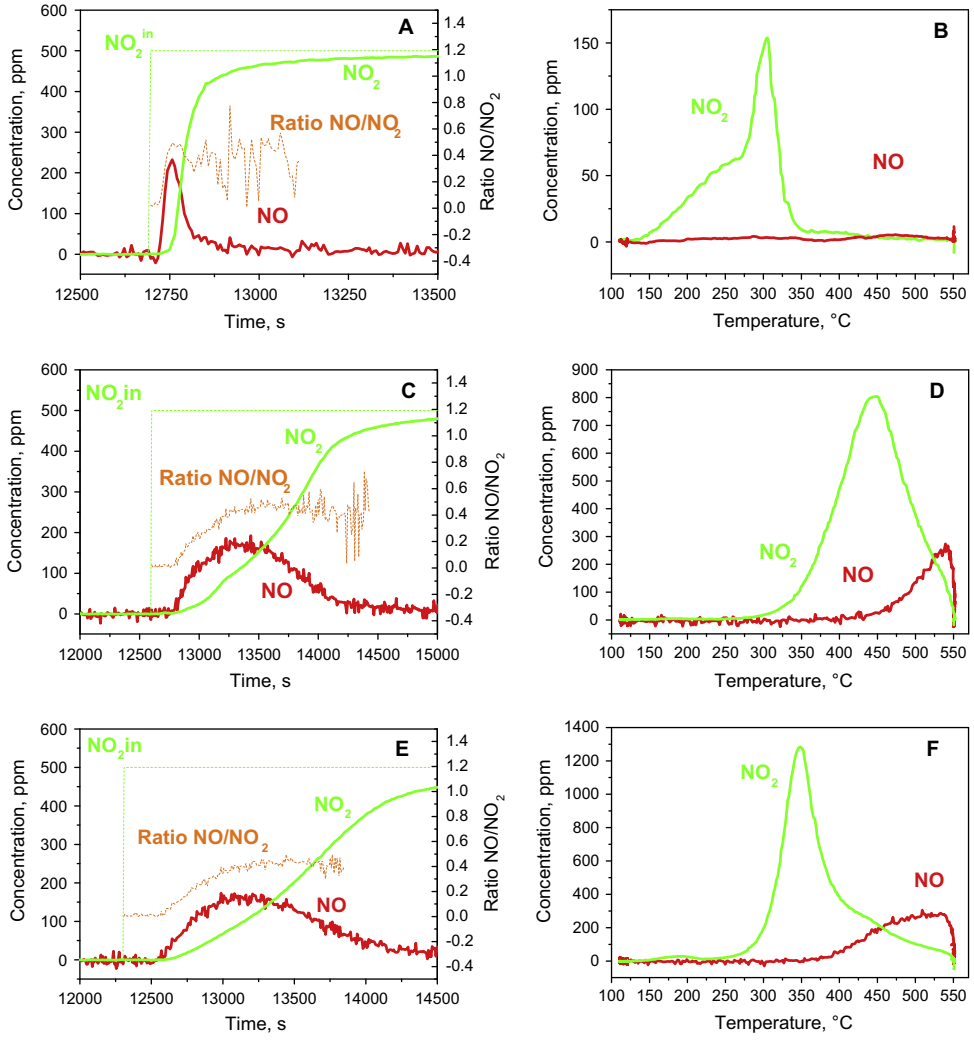

Fig. 2. NO_2 adsorption at 120 °C; Q = 120 cm^3/min (STP); feed: H_2O = 0%; O_2 = 8%; NO_2 = 500 ppm on (A) Fe-ZSM-5 sample, (C) BaO/Al_2O_3 sample, (E) Fe-ZSM-5 + BaO/Al_2O_3 mechanical mixture. Subsequent TPD run: T = 120–550 °C; heating rate = 15 °C/min; feed: H_2O = 0%; O_2 = 0% on (B) Fe-ZSM-5 sample, (D) BaO/Al_2O_3 sample, (F) Fe-ZSM-5 + BaO/Al_2O_3 mechanical mixture.

obtained during the TPD runs over the two individual components. This is evidence that in the case of the BaO/Al_2O_3–Fe-ZSM-5 mixture the decomposition of barium nitrates is assisted by the presence of Fe sites. Again, the decomposition of NO_2 to NO and O_2 takes place only at high temperatures (T > 450 °C).

The lower decomposition temperature of Ba-nitrates in the mechanical mixture could be explained by assuming the existence of an equilibrium between nitrate adspecies and nitric acid in the gas phase. In fact, the nitrates formed on Fe-ZSM-5 are decomposed at a much lower temperature, as shown in Fig. 2B: on increasing the temperature, the equilibrium between nitrates on BaO/Al_2O_3 and HNO_3 is shifted toward the gas phase, and nitric acid adsorbs onto empty Fe sites, forming less stable iron nitrates, which rapidly decompose to NO_2. The participation of HNO_3 in the mechanism of NO_2 disproportionation on Fe-ZSM-5 has been proposed by other authors to interpret the results of in situ FTIR studies [8,12,20]. An alternative explanation could rely on an effect similar to the one invoked for Pt/BaO-based LNT systems [31,32], where spillover of NO_x from BaO to Pt, the active element, has been proposed. In fact, due to the conditioning procedure adopted for the tested samples [21], a direct solid-state interaction between the Fe-zeolite and the BaO/Al_2O_3 phase cannot in principle be excluded in our runs. In this respect, since the inner microporous space of a ZSM-5 zeolite is completely out of reach of the second phase, BaO/Al_2O_3, a direct interaction between Fe sites in the zeolite and the NO_x species accumulated on the BaO surface hardly seems feasible. An alternative possibility is that the conditioning at 600 °C for 5 h may result in a migration of iron species onto the BaO/Al_2O_3 phase of the mechanical mixture, where they come into contact with the adsorbed nitrates. While further clarification of this aspect is needed, in the following we will mostly invoke the gas phase pathway to discuss the Fe-ZSM-5–BaO interaction.

3.2.2. NO_2 adsorption + NO-TPSR

Additional evidence on the nature of the NO_x species stored upon NO_2 exposure has been obtained by TPSR experiments in NO. During the TPSR after the isothermal NO_2 adsorption at 120 °C, 500 ppm of NO are fed stepwise to the reactor at a constant temperature of 120 °C and, once the concentration profiles reach a stationary condition, the temperature is increased at 15 °C/min up to 550 °C in order to probe the reactivity of the adsorbed species with NO. Fig. 3 displays the results of this experiment performed on the Fe-ZSM-5 powdered catalyst sample (Fig. 3A and B), on the BaO/Al_2O_3 NO_x trap (Fig. 3C and D), and on their physical mixture (Fig. 3E and F), respectively.

In particular, Fig. 3A shows the transient at 120 °C after NO is fed stepwise into the reactor loaded with the Fe-ZSM-5 sample. The NO_2 concentration profile rapidly reaches a peak, while

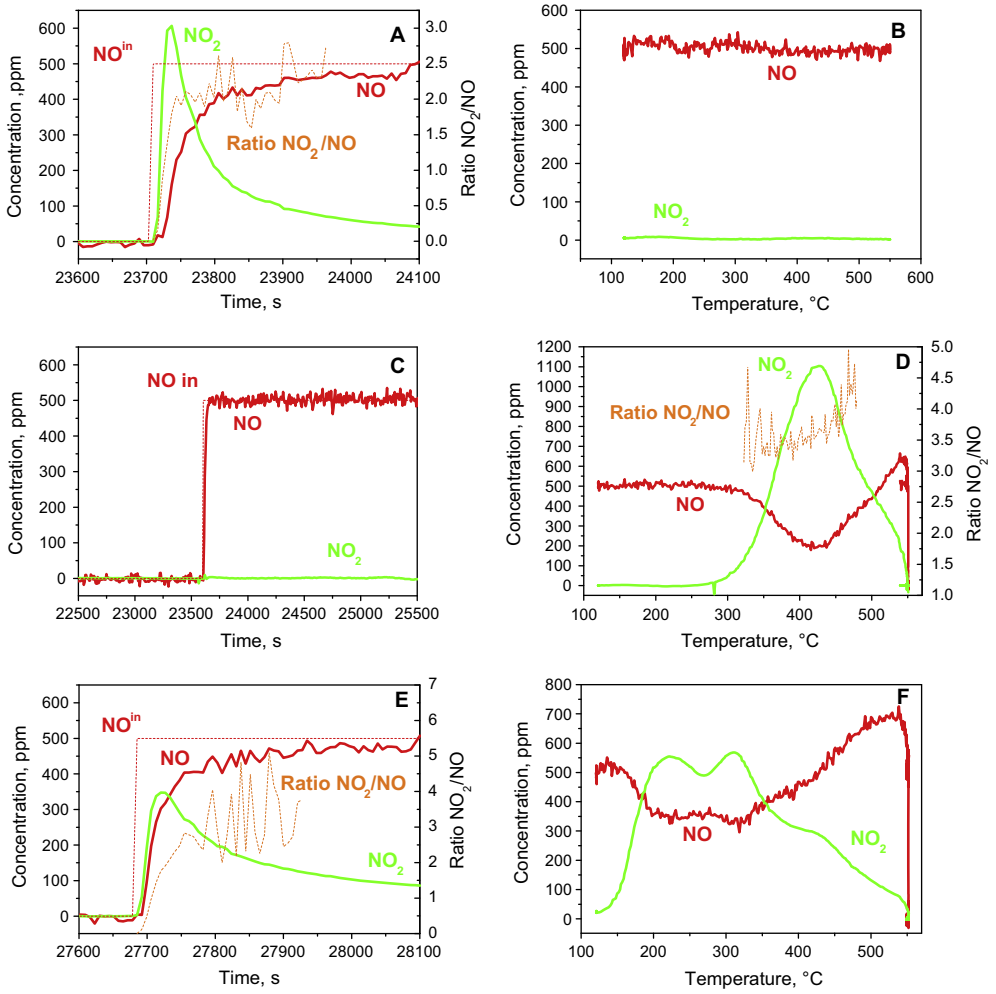

Fig. 3. NO pulse after isothermal NO_2 adsorption at T = 120 °C; Q = 120 cm^3/min (STP); feed: H_2O = 0%; O_2 = 0%; NO = 500 ppm on (A) Fe-ZSM-5 sample, (C) BaO/Al_2O_3 sample, (E) Fe-ZSM-5 + BaO/Al_2O_3 mechanical mixture. Subsequent TPSR run: T = 120–550 °C; heating rate = 15 °C/min; feed: H_2O = 0%; O_2 = 0%; NO = 500 ppm on (B) Fe-ZSM-5 sample, (D) BaO/Al_2O_3 sample, (F) Fe-ZSM-5 + BaO/Al_2O_3 mechanical mixture.

correspondingly the NO trace starts to grow, approaching a steady state after 200 s. The ratio between the released NO_2 and consumed NO (Fig. 3A) approaches 2, indicating that NO is likely able to reduce nitrates adsorbed onto the oxidized Fe-zeolite according to the mechanism [27]

$$NO_{(g)} + Fe^{3+}(NO_3^-) \leftrightarrow NO_{2,(g)} + Fe^{3+}(NO_2^-), \quad (R.8)$$

$$Fe^{3+}(NO_2^-) \rightarrow NO_{2,(g)} + Fe^{2+}, \quad (R.9)$$

which adds up to

$$NO_{(g)} + Fe^{3+}(NO_3^-) \rightarrow 2NO_{2,(g)} + Fe^{2+}. \quad (R.10)$$

In the following stage of the run, shown in Fig. 3B, the temperature is progressively increased while still feeding NO to the reactor: however, neither significant desorption of NO_2 nor NO consumption is observed, a clear indication that all the nitrates have been reduced already at 120 °C. The integral of stored nitrates corresponds, with an error of about 2%, to half the overall amount of NO_2 released during the nitrates reduction phase at 120 °C, as well as to the amount of NO consumed in the same step, nicely in line with the stoichiometry of (R.10).

The same experiment performed on BaO/Al_2O_3 gives different results (Fig. 3C and D). First, when NO is fed into the reactor at 120 °C, nothing significant takes place: NO is unable to reduce surface nitrates on BaO/Al_2O_3 at this temperature (Fig. 3C). Second, unlike the case in Fig. 3B, in which NO_2 is absent, during NO TPSR a NO_2 peak is noticed at 425 °C in Fig. 3D. This peak occurs at a lower temperature (425 °C vs. 450 °C) than for nitrates desorption observed during TPD experiments (Fig. 2D), so in this case the NO_2 evolution does not result simply from thermal decomposition of nitrates. Moreover, significant NO conversion is measured in the same temperature range. Based on such evidence we conclude that, starting from 300 °C, NO is consumed to reduce nitrates species to NO_2 according to the reaction

$$Ba(NO_3)_2 + NO_{(g)} \rightarrow BaO + 3NO_{2,(g)}. \quad (R.11)$$

The estimation of the NO_2/NO ratio, slightly higher than 3, as plotted in Fig. 3D, suggests that, besides nitrate reduction by NO, nitrate thermal decomposition also occurs in this high temperature range, as confirmed by TPD experiments. Decomposition of NO_2 to NO and O_2 at high temperatures is also present. The integral balance of N species is closed within 5%, comparable to the experimental accuracy.

Fig. 3E and F illustrate the same experiment performed on the mechanical mixture comprising both Fe-ZSM-5 and BaO/Al_2O_3. Again, NO is able to reduce nitrates on the Fe-zeolite at 120 °C, as apparent in Fig. 3E. Initially, when the NO_2 outlet concentration reaches a maximum at around 350 ppm, the NO_2/NO molar ratio approaches 2, meaning that the same mechanism described by

(R.8)–(R.10) applies, but then it tends to oscillate around 3. This can be explained assuming that

$$2NO^{-}_{3,(ads)} + NO_{(g)} \leftrightarrow 3NO_{2,(g)} + O^{2-}_{(ads)}. \quad \text{(R.3rev)}$$

When the temperature is raised during the NO TPSR, a peculiar M-shaped NO_2 concentration profile is observed: a first NO_2 peak is noticed at 225 °C, then at 270 °C we pass through a minimum, and new peaks at 310 °C and 425 °C are apparent. The NO concentration profile mirrors the NO_2 profile up to 350 °C, where the decomposition of NO_2 to NO and O_2 starts to be significant. In this case also, the integral balance of N species is closed with a 5% error.

The behavior during NO TPSR in Fig. 3F can be explained by considering again the existence of surface species/gas-phase equilibria. In particular, if we assume that ferric nitrates on Fe-ZSM-5 are completely reduced at 120 °C, as indicated by Fig. 3A and B, empty Fe sites could act as additional decomposition sites for barium nitrates via gas phase HNO_3/NO_2, thus originating the NO_2 peaks at 225 °C and 310 °C. With further increase in the temperature, nitrates begin to be reduced directly on BaO/Al_2O_3, giving rise to the NO_2 peak at 425 °C. Again, however, direct NO_x migration via solid-state Fe–BaO interaction cannot be excluded.

3.2.3. NO_2 adsorption + ex situ IR analysis

To conclude the examination of the NO_2 reacting system, an ex situ IR spectroscopic analysis is performed to further confirm the nature of the species stored during NO_2 adsorption on the three investigated systems. Fig. 4 compares FTIR spectra collected on the Fe-ZSM-5 and BaO/Al_2O_3 samples unloaded from the test reactor after exposure to NO_2 and O_2 at 120 °C.

The spectra in Fig. 4A were recorded on Fe-ZSM-5 separated from a mechanical mixture with BaO/Al_2O_3, while the data in Fig. 4B were obtained on an individually tested Fe-ZSM-5 sample. The two spectra show similar features, with a main peak at 1630 cm^{-1} assigned to ferric nitrates (Fe(III)NO_3) [5,12]. Moreover, a small peak at 1875 cm^{-1}, assigned to nitrosyl species (Fe(II)NO) [12], can be noticed. Interestingly, the results obtained in the present ex situ FTIR analysis are in line with those reported in the in situ FTIR study of NO_2 adsorption performed by Ruggeri et al. [12] on the same Fe-ZSM-5 catalyst, which showed ferric nitrates to be the primary stable adspecies at steady state after a pulse of NO_2. For the implications of such features for the mechanism of NO_2 adsorption, we refer to the systematic in situ FTIR investigation illustrated in [12].

The spectrum in Fig. 4C was collected on BaO/Al_2O_3 separated from a mechanical mixture with Fe-ZSM-5, while the spectrum in Fig. 4D was obtained from a BaO/Al_2O_3 sample tested individually. In both spectra we identify a main peak at 1380 cm^{-1}, which, based on several literature reports [33,34], may be assigned to free nitrate ions deriving from transformation of different surface nitrate species possibly involving the presence of gas-phase HNO_3, as previously proposed to explain the interaction between the two components of the mechanical mixture. Another peak at 1410 cm^{-1} may be assigned to ionic nitrates [35]. In the case of the individual barium sample (Fig. 4D), an additional peak at 1350 cm^{-1} assigned to chelating nitrites [24] is present. For both BaO/Al_2O_3 and Fe-ZSM-5, the differences between IR spectra collected on individually tested samples and on mechanical mixture components may be related to the adopted operative procedures. In particular, for the mechanical mixture samples, a few days typically passed between the exposure to NO_2 and the ex situ IR analysis: for this reason, some adsorbed species may have undergone transformations. Fig. S1 in the Supporting Material indicates, however, that ex situ FTIR measurements replicated on the same samples after 6 weeks showed no modifications in the detected bands, except for an increased intensity of the band at 1380 cm^{-1} assigned to free nitrate ions. This can be regarded as an additional indication of a possible equilibrium between nitrate adspecies and nitric acid, as previously proposed [8,20].

By comparing the FTIR analyses of the components of the mechanical mixture and of the single phases it is possible to exclude once more any synergy during the adsorption phase. In

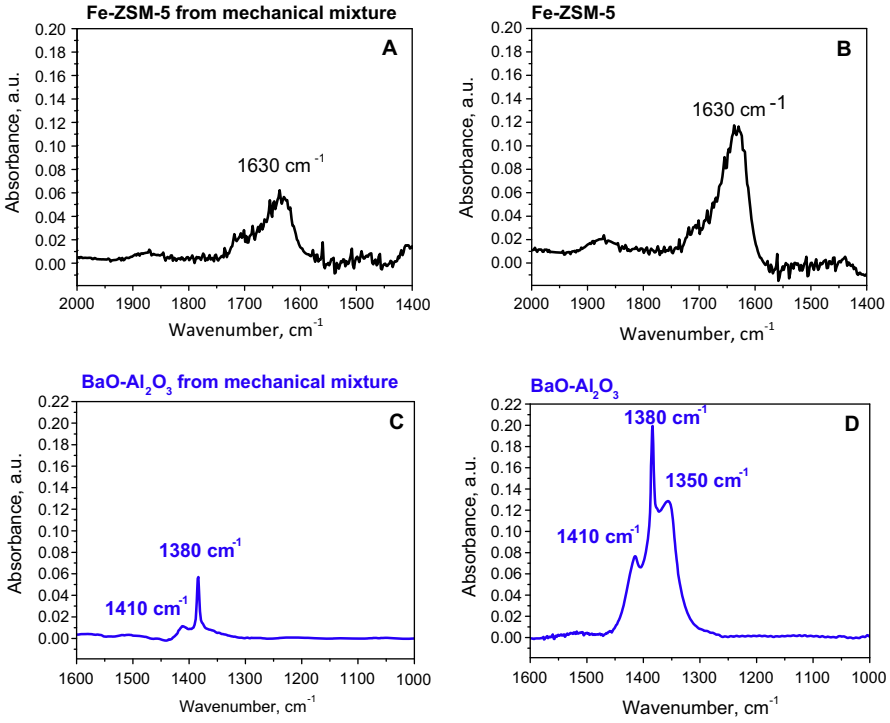

Fig. 4. NO_2 adsorption at 120 °C: ex situ IR analysis. T = 120 °C; Q = 120 cm^3/min (STP); feed: H_2O = 0%; O_2 = 8%; NO_2 = 500 ppm. (A) Fe-ZSM-5 component from the mechanical mixture, (B) Fe-ZSM-5 individual sample, (C) BaO/Al_2O_3 component from the mechanical mixture, (D) BaO/Al_2O_3 individual sample.

fact, except for some limited differences due to the experimental procedures, the species stored by the two individual phases and by the two phases combined in the mixture are essentially the same.

In summary, the NO_2 adsorption study on the Fe-ZMS-5 catalyst has shown no especially novel results, confirming the storage of relatively stable ferric nitrates. It lends confidence, however, to the experimental approach adopted here, the results being in line with a number of previous literature reports. This is the case, for example, for similarity of the indications obtained from the ex situ FTIR analysis to in situ FTIR literature studies. Furthermore, we have validated our experimental approach demonstrating not only the possibility to trap NO_x species on the BaO/Al_2O_3 phase of the physical mixture, but also, more importantly, to identify interactions between the two component phases.

In the following we apply the same chemical trapping methods to investigate the more controversial interaction of NO with Fe-ZSM-5.

3.3. $NO + O_2$ adsorption

After establishing the behavior of NO_2 when it interacts with the three catalytic systems under study, we proceed now to analyze the results obtained when, instead of NO_2, NO is fed to the reactor in the presence of O_2. The same protocol as adopted for NO_2 is followed: first, we perform isothermal adsorption experiments at 120 °C with 500 ppm of NO and 8% v/v O_2, followed by TPD to assess the nature of the adspecies by looking at their decomposition products. Then the reactivity of such adspecies is probed in a TPSR run, feeding in this case 500 ppm of NH_3, i.e., a situation representative of the standard SCR reaction. To gain further insight into the SCR mechanism, an additional dual experiment is run on the mechanical mixture only, namely adsorption of 500 ppm of NH_3 at 120 °C on the Fe-ZSM-5 + BaO/Al_2O_3 followed by a TPSR with 500 ppm of NO and 8% v/v O_2. Finally, ex situ FTIR analysis of both Fe-ZSM-5 and BaO/Al_2O_3 is performed after $NO + O_2$ adsorption in order to conclusively identify the adsorbed species.

3.3.1. $NO + O_2$ adsorption + TPD

Fig. 5A shows the isothermal $NO + O_2$ adsorption phase for the Fe-ZSM-5 catalyst sample diluted with cordierite. The NO outlet concentration trace exhibits extremely limited delay relative to the NO inlet profile. The behavior is very similar to blank tests performed in an empty reactor and in a reactor loaded with bare cordierite powder (not reported, for brevity), which showed just a

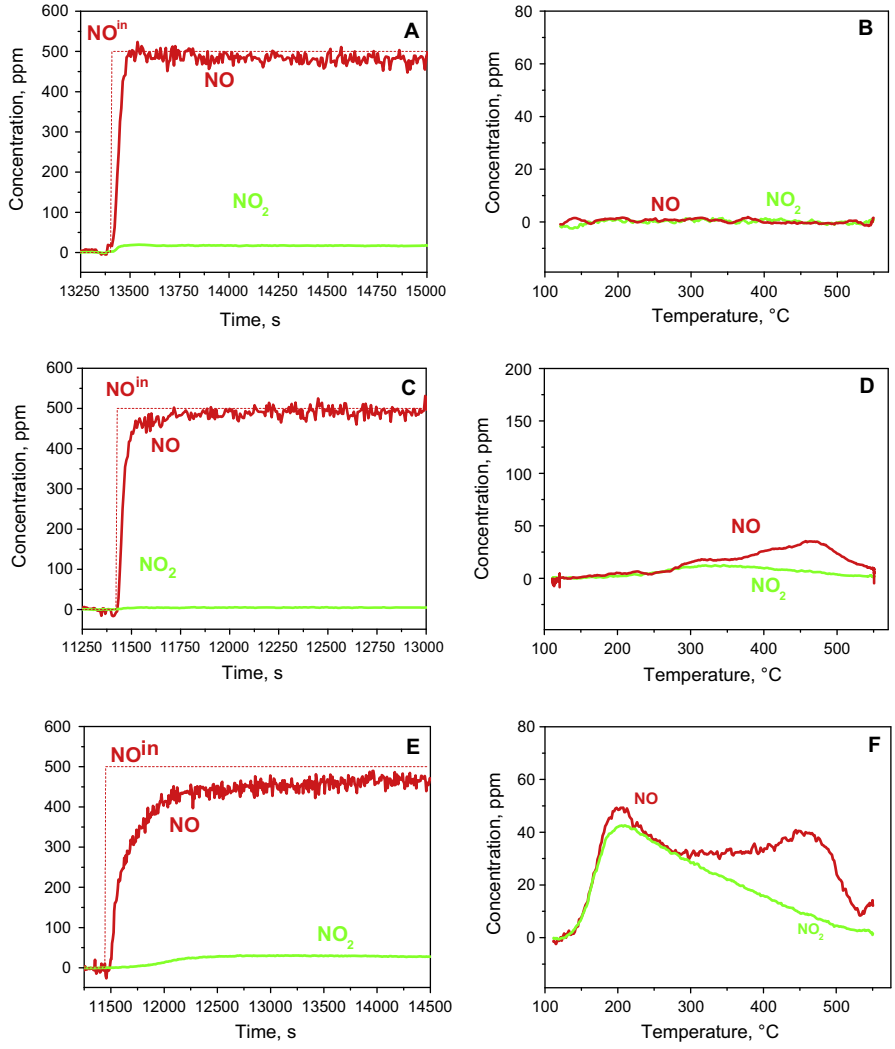

Fig. 5. $NO + O_2$ adsorption at 120 °C; $Q = 120$ cm^3/min (STP); feed: $H_2O = 0\%$; $O_2 = 8\%$; NO = 500 ppm on (A) Fe-ZSM-5 sample, (C) BaO/Al_2O_3 sample, (E) Fe-ZSM-5 + BaO/Al_2O_3 mechanical mixture. Subsequent TPD run: $T = 120$–550 °C; heating rate = 15 °C/min; feed: $H_2O = 0\%$; $O_2 = 0\%$ on (B) Fe-ZSM-5 sample, (D) BaO/Al_2O_3 sample, (F) Fe-ZSM-5 + BaO/Al_2O_3 mechanical mixture.

limited amount of physisorbed NO. The NO outlet concentration dynamics are very fast, approaching steady state after only 100 s. In addition, simultaneous NO_2 evolution is observed: NO_2 exhibits a dead time of around 25 s, and then its concentration slowly grows to about 20 ppm at steady state, indicating modest NO oxidation activity, in line with previous studies [13]. Fig. 5B presents the TPD run for the same sample, showing no significant desorption. Thus we conclude that NO is not stored in appreciable quantities on the Fe-zeolite catalyst, in line with other experimental evidence in the literature [26,28]. At this low temperature (120 °C), the potential intermediate adspecies involved in NO oxidation should be formed in significant amounts on Fe-ZSM-5, but they are likely very unstable and thus it is impossible for them to be stored and detected during the following TPD.

Fig. 5C shows isothermal NO + O_2 adsorption on the BaO/Al_2O_3 phase diluted with cordierite. The NO concentration profile is associated with slightly more pronounced dynamics, reaching a steady state after approximately 300 s. Moreover, extremely limited (just a few ppm) NO_2 evolution is observed in this case, meaning that the NO oxidation activity over BaO/Al_2O_3 is almost negligible, as expected [35]. The corresponding TPD results for the BaO/Al_2O_3 phase, Fig. 5D, show very modest initial equimolar desorption of NO and NO_2 until 300 °C and, at higher temperatures, a NO broad peak likely due to the onset of NO_2 decomposition to NO + O_2. The integral of the NO_x stored during the adsorption phase differs from the total NO_x desorbed during the TPD by ~10%. The moles of desorbed NO_x (0.0047 $mmol_{NOx}$) correspond to about 1.8% of the overall number of BaO sites. This confirms that BaO/Al_2O_3 is able to effectively trap possible NO_x species originated upon exposure of the sample to NO and O_2. In this experiment over the individual BaO/Al_2O_3 phase, however, the formation of such species was almost negligible.

Finally, Fig. 5E shows the isothermal NO + O_2 adsorption phase for the mechanical mixture of Fe-ZSM-5 and BaO/Al_2O_3. This test has been replicated and confirms the preliminary results already reported in [21]. The situation here is quite different from that in Fig. 5A–D. The NO outlet concentration profile shows a delay of around 25 s relative to the NO inlet trace. Moreover, the NO outlet concentration dynamics are very slow compared to the previous two cases, approaching steady state only after over 2000 s. In addition, steady-state NO conversion with NO_2 evolution is observed: NO_2 exhibits a dead time of over 200 s, and then its concentration grows slowly to a stationary level of about 30 ppm, slightly higher than that obtained by summing the oxidation activities observed on the two single phases [21].

The TPD results for the physical mixture in Fig. 5F show simultaneous desorption of NO and NO_2 in approximately equimolar amounts up to 250 °C (confirmed by both the UV analyzer and the MS), with a maximum at 200 °C. Notably, the thermal stability of adsorbed species is already critical at 120 °C, NO_x being desorbed as soon as the temperature is increased. At higher temperatures (370 °C), we notice the onset of NO_2 decomposition to NO + O_2, likely proceeding on Fe sites in this case. In line with [21], the integrals of stored and desorbed NO_x (0.0122 $mmol_{NOx}$) are in satisfactory agreement and the occupation of Ba sites (13%) is consistent with data reported in the LNT literature [29,35]. Notice that the overall amount of NO_x stored on the Fe-ZSM-5 + BaO/Al_2O_3 mixture is by far higher than the sum of the NO_x stored on the two individual components, indicating a strong positive interaction between the two phases during NO + O_2 adsorption.

As already pointed out in our previous communication [21], the evolution of NO and NO_2 in equimolar amounts at low temperatures (Fig. 5F) is strongly suggestive of the thermal decomposition of nitrites. We further discuss the nature of the stored NO_x species in the following sections, after introducing additional data.

3.3.2. NO + O_2 adsorption + NH_3 TPSR

To assess the nature of the NO_x species adsorbed on the mechanical mixture, we have performed an additional set of experiments involving TPSR with NH_3, as detailed at the beginning of this section. The adopted feed conditions are typical of the standard SCR reaction and thus useful to better understand its low-temperature mechanism. The first part of the experiment (isothermal NO + O_2 adsorption phase at 120 °C) will be omitted, being a replication of those already discussed (Fig. 5A, C, and E) and only the results related to the subsequent NH_3 TPSR part will be discussed in the following. Furthermore, nothing significant takes place on the individual Fe-ZSM-5 sample since, as depicted in Fig. 5A and B, no storage occurs. Similar considerations hold also for the BaO/Al_2O_3 sample, where an extremely limited storage, Fig. 5C and D, is observed and nothing meaningful is obtained during the NH_3 TPSR. For these reasons only the results relating to the NH_3 TSPR on the mechanical mixture will be presented and discussed; see Fig. 6.

A first important result in Fig. 6A is the appearance of a N_2 peak of approximately 80 ppm some time after ammonia is fed to the reactor, but still at the initial constant temperature of 120 °C. This is clear evidence supporting the presence of adsorbed nitrites: in fact, their low-temperature reactivity with ammonia to form N_2 via decomposition of unstable NH_4NO_2 is well known [1,5,8]. On the other hand, nitrates are not reactive with NH_3 in the 120–200 °C interval [3]. However, as shown in Fig. 5A and B, nitrites should not be present on Fe-ZSM-5, being unstable at 120 °C. This means that the N_2 peak in Fig. 6A should be attributed to the reaction of nitrites stored on barium with ammonia. In particular, two different reaction mechanisms are possible: in the first, gaseous NH_3 reacts directly with nitrites stored on BaO; in the second, gaseous nitrous acid at equilibrium with the nitrites adspecies is intercepted by adsorbed ammonia, e.g., in the form of

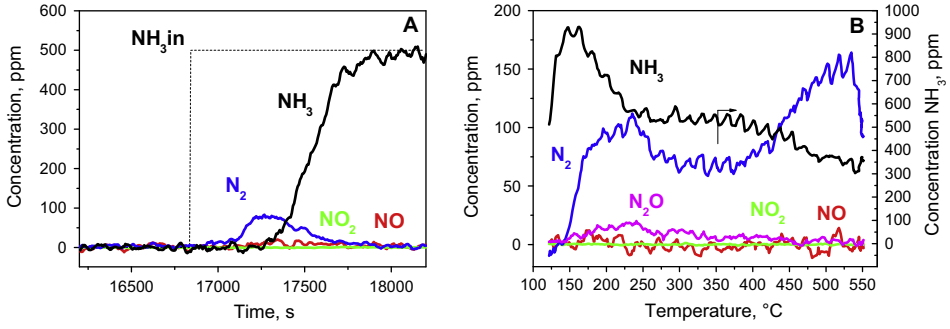

Fig. 6. NH_3 TPSR after NO + O_2 adsorption at 120 °C on the Fe-ZSM-5 + BaO/Al_2O_3 physical mixture. (A) NH_3 pulse at 120 °C. T = 120 °C; Q = 120 cm^3/min (STP); feed: H_2O = 0%; O_2 = 0%; NH_3 = 500 ppm. (B) Subsequent TPSR run: T = 120–550 °C; heating rate = 15 °C/min; feed: H_2O = 0%; O_2 = 0%; NH_3 = 500 ppm.

ammonium ions formed on Fe-ZSM-5. In both cases, the final reaction products are N_2 and H_2O,

$$Ba(NO_2)_2 + 2NH_{3,(g)} \rightarrow BaO + 2N_{2,(g)} + 3H_2O_{(g)}, \quad (R.12)$$

or alternatively

$$HONO_{(g)} + Z{-}NH_{4,(ads)} \rightarrow N_{2,(g)} + 2H_2O_{(g)} + Z{-}H. \quad (R.13)$$

When the temperature increases (Fig. 6B), additional nitrogen is produced, likely due to the reaction of other more stable nitrites with ammonia. Heterogeneity of nitrite adspecies is supported both by the TPD profiles shown in Fig. 5F and by the ex situ FTIR spectra (see *NO + O_2 adsorption + ex situ IR analysis*).

Finally, an additional N_2 peak is noted at high temperature, which may be ascribed to the onset of the reaction of NH_3 with surface nitrates [13]. A small production of N_2O, on the order of 20 ppm, is observed as well due to the reaction of NH_3 with NO_2.

To discriminate between (R.12) and (R.13) as the mechanism of the reaction between NH_3 and nitrites, a dual TPSR experiment between preadsorbed NH_3 and NO + O_2 is performed on the Fe-ZSM-5 + BaO/Al_2O_3 physical mixture, as detailed at the beginning of this section, with results reported in Fig. 7. In particular, Fig. 7A shows a long delay (about 450 s) in the ammonia concentration profile. This indicates considerable storage of NH_3 on the mechanical mixture, estimated to be about 0.023 mmol of strongly bonded ammonia, which is consistent with the NH_3 storage capacity of Fe-zeolites reported in the literature [26]. The most interesting result is obtained during the following part of the experiment, shown in Fig. 7B. As soon as NO and O_2 are fed to the reactor, still at 120 °C, a significant N_2 peak is observed, with a maximum of approximately 250 ppm. Notably, nitrogen release takes place with no appreciable delay with respect to the NO signal, differently from what happens, for example, in Fig. 6A. This is an indication that the standard SCR reaction at low temperature proceeds between adsorbed ammonia and nitrites, which are immediately formed as soon as NO and O_2 are fed to the Fe catalyst, possibly according to the mechanism proposed in reaction (R.13), which involves gaseous HONO. On the other hand, the alternative mechanism, i.e., the reaction between NH_3 in gas phase and stored nitrites, (R.12), is hardly compatible with the results in Fig. 7B, as well as with the delay observed in Fig. 6A, where nitrites are available at the chemical trap surface and NH_3 in gas phase is being fed to the reactor.

During the temperature ramp in the last part of the run, shown in Fig. 7C, no evolution of N_2 and NH_3 is noted, indicating that all the preadsorbed ammonia has reacted with nitrites already at 120 °C, which is confirmed by the integral N-balance. The dynamics of NO and NO_2 apparent in Fig. 7C result from the decomposition of nitrites formed from NO + O_2 after the consumption of all the adsorbed ammonia until about 170 °C. Above that temperature the oxidation of NO to NO_2 starts to take place until the onset of temperatures favorable to NO_2 decomposition, as already discussed in previous sections.

3.3.3. *NO + O_2 adsorption + ex situ IR analysis*

To conclude the study of the NO + O_2 reacting system, ex situ IR spectroscopic analyses have been performed to further confirm the identification of the species stored during NO adsorption. Dedicated tests were performed for this purpose, where only the isothermal NO + O_2 adsorption at 120 °C was replicated: at the end of this phase the powdered sample (not diluted with cordierite in this case) was unloaded from the reactor and sent to the IR analyzer. In the case of the Fe-ZSM-5 + BaO/Al_2O_3 mixture the two phases were separated by sieving [21]. Fig. 8 shows ex situ FTIR spectra recorded on the unloaded Fe-ZSM-5 and BaO/Al_2O_3 powders after exposure to NO + O_2.

First it is worth noticing the differences between spectra obtained on the Fe-ZSM-5 sample separated from the mechanical mixture, Fig. 8A, and on the individually tested Fe-ZSM-5 sample, Fig. 8B. In particular, on the latter sample, features at 1640 and 1384 cm^{-1} are evident that can be assigned to ferric nitrates [12] and free nitrate ions [33,34], respectively. It seems evident that, even if in limited amounts, nitrates are present on the individually

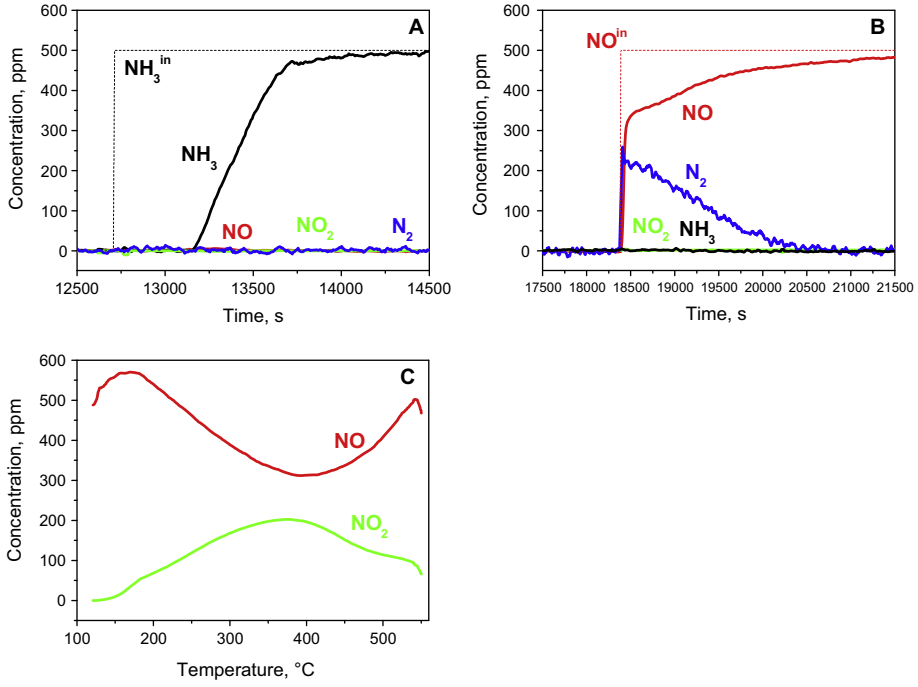

Fig. 7. (A) NH_3 adsorption at 120 °C on the Fe-ZSM-5 + BaO/Al_2O_3 sample. T = 120 °C; Q = 120 cm^3/min (STP); feed: H_2O = 0%; O_2 = 0%; NH_3 = 500 ppm. (B) Subsequent NO + O_2 pulse at 120 °C. T = 120 °C; Q = 120 cm^3/min (STP); feed: H_2O = 0%; O_2 = 8%; NO = 500 ppm. (C) Subsequent TPSR run: T = 120–550 °C; heating rate = 15 °C/min; feed: H_2O = 0%; O_2 = 8%; NO = 500 ppm.

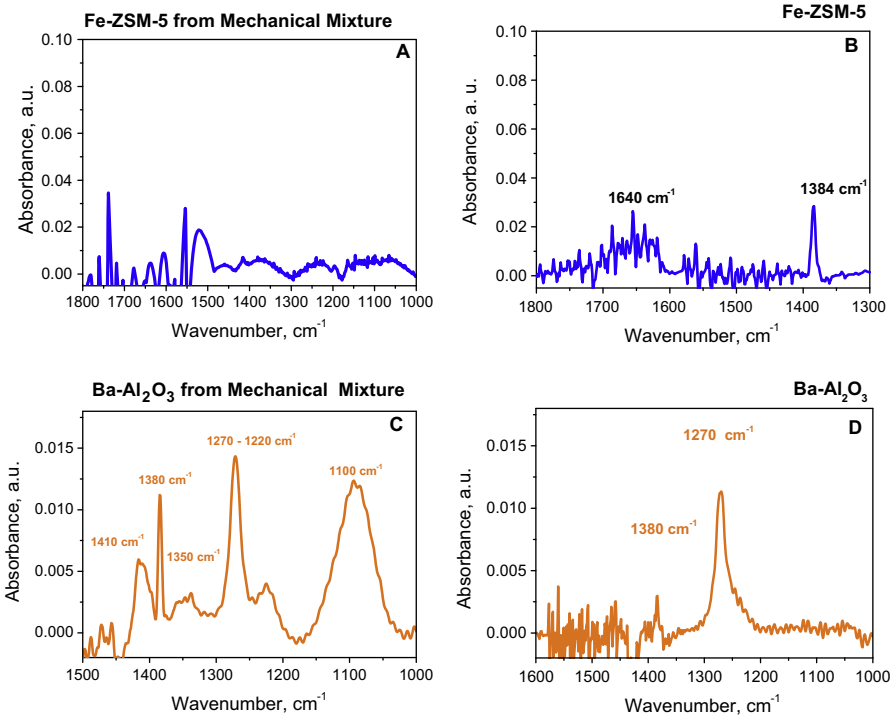

Fig. 8. NO + O_2 adsorption at 120 °C: ex situ IR analysis. T = 120 °C; Q = 120 cm^3/min (STP); feed: H_2O = 0%; O_2 = 8%; NO = 500 ppm. (A) Fe-ZSM-5 component from the mechanical mixture, (B) Fe-ZSM-5 individual sample, (C) BaO/Al_2O_3 component from the mechanical mixture, (D) BaO/Al_2O_3 individual sample.

tested Fe-zeolite sample after exposure to NO + O_2. This is in line with the results of previous in situ FTIR studies on the same material [20].

Fig. 8A shows, however, that this is not the case for the Fe-ZSM-5 sample separated from the mechanical mixture, where essentially no adsorbed species are detected. This is consistent with nitrates being formed on Fe-ZSM-5 consecutive to nitrites: oxidation of nitrites is hindered when BaO is present, nitrites being trapped and stored in a stable, less reactive form.

For BaO/Al_2O_3, significant differences between the spectra recorded on the sample separated from the mechanical mixture, Fig. 8C, and on the individually tested sample, Fig. 8D, are evident, too. Due to the synergy between the two phases, many more different adspecies are detected by IR on the former sample while, due to the negligible NO oxidation activity of BaO/Al_2O_3, only small amounts of nitrites are detected on the latter sample. In particular, in Fig. 8C we observe a main band around 1100 cm^{-1} that can be assigned to ν_{N-O} modes of Ba nitrites [36,37]. The band at 1220 cm^{-1} is representative of nitrite adspecies and, more precisely, of the ν_{asym} of NO_2 associated with ionic nitrites [24,34–36]. The most interesting feature is represented by the peak at 1270 cm^{-1}, which can be assigned to free NO_2^- [8,34,38,39]. The presence of free nitrite ions may originate from the transformation of different adsorbed nitrites, and could suggest the existence of an equilibrium between such adspecies and HONO in the gas phase, similarly to what happens for nitrates. The 1350 cm^{-1} band is assigned to chelating nitrites according to [24]. Traces of nitrates are also present, as indicated by the band at 1410 cm^{-1}, which is assigned to $\nu_{NO3,sym}$ of ionic nitrates [35].

In conclusion, the ex situ FT-IR analysis confirms what was already suggested by the transient response experiments: the oxidative activation of NO over Fe-ZSM-5 at low temperatures, as required in the mechanisms of NO oxidation to NO_2 and of standard SCR, proceeds through initial formation of nitrites, possibly in equilibrium with HONO. The role of nitrates as primary intermediates for the low-T standard SCR reaction can be excluded.

3.4. Mechanistic considerations

The results shown in Figs. 5–7 are nicely explained by the redox mechanism already proposed for NO oxidation to NO_2 over Fe-zeolites [21] and reported here for completeness. In this mechanism we assume the active centers to be monomeric hydroxylated ferric sites [40]. This hypothesis seems reasonable since, as confirmed by results reported in the Supporting Material, Fig. S2, desorption of residual water from the zeolite was detected also in the TPD experiments performed under reference dry conditions, though in much smaller amounts than in control experiments under wet conditions, also presented in Fig. S2. We conclude therefore that a certain amount of bound water is always present on the Fe-zeolite even after the dry pretreatment procedure.

Starting from the catalyst in an oxidized state, we propose that the following reaction steps hold at low temperature:

$$Fe^{3+}OH + NO_{(g)} \leftrightarrow Fe^{2+} + HONO_{(g)}, \quad (R.14)$$

$$HONO_{(g)} + Fe^{3+}OH \leftrightarrow Fe^{3+}ONO + H_2O_{(g)}, \quad (R.15)$$

$$Fe^{3+}ONO \rightarrow Fe^{2+} + NO_{2,(g)}, \quad (R.16)$$

$$2Fe^{2+} + \frac{1}{2}O_{2,(g)} + H_2O_{(g)} \rightarrow 2Fe^{3+}OH, \quad (R.17)$$

$$Fe^{3+}ONO + NO_{2,(g)} \rightarrow Fe^{3+}NO_3 + NO_{(g)}. \quad (R.18)$$

NO oxidation proceeds in two stages ((R.14)–(R.17)) to form ferric nitrites, which may be in equilibrium with gaseous HONO (R.14). This possible equilibrium, besides explaining the well-known strong H_2O inhibitory effect on NO oxidation [9,13], as discussed in [21], accounts properly for the reported experimental results. In fact, as we show in Fig. 5C, the NO oxidation activity over BaO/Al_2O_3 is negligible [35] with a subsequent very limited NO_x adsorption (one order of magnitude less than on the physical mixture; see Fig. 5C and E). In addition, adsorption of nitrites at 120 °C is found to be insignificant on Fe-ZSM-5, Fig. 5A, due to the high reactivity and instability of the nitrites formed through reaction

(R.15). However, the combination of these two systems in a physical mixture gives rise to a significant synergistic effect with considerable storage of barium nitrite species, Fig. 5E. In this case, in fact, gaseous HONO formed by NO oxidation over Fe sites in step (R.14) can interact either with another oxidized Fe site or with BaO storage sites (more abundant, as described in Section 2) to form Fe–ONO or $Ba(NO_2)_2$ according to (R.15) or the following reaction, respectively:

$$BaO + 2HONO_{(g)} \leftrightarrow Ba(NO_2)_2 + H_2O_{(g)}. \quad (R.19)$$

Step (R.19) would be thus responsible for the formation of stable nitrites on Ba. The existence of this equilibrium between Fe-nitrites and Ba-nitrites via gaseous HONO also explains the peculiar dynamics apparent in Fig. 5E, where the NO_2 product takes a significant amount of time to break through, as detailed in [21], nitrites being accumulated onto BaO/Al_2O_3. The TPD results shown in Fig. 5D and F may be explained by the decomposition of stable Ba-nitrites via gaseous HONO according to the steps [41]

$$Ba(NO_2)_2 + H_2O_{(g)} \leftrightarrow BaO + 2HONO_{(g)}, \quad (R.19rev)$$

$$2HONO_{(g)} \rightarrow NO_{(g)} + NO_{2,(g)} + H_2O_{(g)}. \quad (R.20)$$

This is well in line with the desorption of NO and NO_2 in equimolar proportions noted in Fig. 5F.

It is worth emphasizing that the trapping of HONO by BaO, preventing further evolution to nitrates according to (R.15), (R.16), and (R.18), also explains the lack of detection of nitrates on the Fe-ZSM-5 sample separated from the physical mixture (Fig. 8A). The results in Fig. 7 further suggest that under standard SCR conditions the same trapping role of the reactive HONO intermediate played by BaO may be played instead by adsorbed NH_3. Instead of stable Ba-nitrites, however, unstable NH_4NO_2 would be formed in this case, which would rapidly decompose to N_2. Limited formation of nitrates from $NO + O_2$ in the presence of NH_3 has been in fact recently reported on Cu-SAPO-34 [19].

Finally, to examine the impact of H_2O, a control experiment (presented and discussed in the Supporting Material, Fig. S2) was performed by feeding a 3% H_2O pulse for 30 s after the isothermal adsorption of $NO + O_2$ at 120 °C. This test showed no modification in the qualitative behavior of the following TPD, during which we again observed equimolar desorption of NO and NO_2 as a result of $Ba(NO_2)_2$ decomposition, like in the "dry" experiments. On the other hand, analysis of the TPD showed in this case a reduced amount of nitrites stored on the BaO/Al_2O_3 phase, thus confirming the inhibitory effect of water on nitrite storage via reactions (R.15) and (R.19) predicted by our mechanism.

4. Conclusions

While nitrites have been often proposed as reactive intermediates in NO oxidation and standard SCR, they had been hardly detected so far over metal-exchanged zeolites. In the present work the preliminary conclusions of our previous study [21] on the primary products of the oxidative activation of NO on an Fe-ZSM-5 catalyst and their role in the mechanisms of NO oxidation to NO_2 and standard SCR are confirmed and expanded by additional results obtained using the same technique, based on mixing Fe-ZSM-5 with BaO/Al_2O_3 as a NO_x trap to intercept, store, and detect otherwise elusive reactive intermediates. Our data for $NO + O_2$ adsorption clearly support that the oxidative activation of NO proceeds at low temperature via nitrite adspecies, formed over Fe-ZSM-5 but captured and stabilized on BaO/Al_2O_3, possibly via gas-phase HONO. The identification of nitrites is confirmed by multiple evidence, namely (i) thermal decomposition of the stored NO_x to an equimolar NO/NO_2 mixture during TPD; (ii) N_2 formation upon reaction of the stored NO_x with NH_3 at low T during NH_3 TPSR; and (iii) ex situ IR analysis of the unloaded and separated BaO/Al_2O_3 phase.

On the other hand, the results from the parallel investigation of NO_2 adsorption presented here rule out nitrates as primary intermediates in NO oxidation at low temperature. In fact, nitrates exhibit different TPD and TPSR behavior than observed during $NO + O_2$ experiments. Furthermore, ex situ IR analysis of the unloaded Fe-ZSM-5 phase indicates that formation of nitrates from $NO + O_2$ is inhibited in the presence of BaO, suggesting that the reactive nitrite intermediates are intercepted by the NO_x trap. We propose that a similar role is played by adsorbed NH_3 under standard SCR conditions. Moreover, it is shown that the preferred pathway for standard SCR at low temperature is likely the reaction of nitrites/HONO with adsorbed ammonia.

The present study seems therefore to support a standard SCR mechanism based on the "nitrite route" [19]. Notably, our data may be also compatible with mechanistic proposals involving NO^+ species as intermediates [10], whose transformation into nitrites can easily be envisaged.

Appendix A. Supplementary material

Supplementary data associated with this article can be found in the online version.

References

[1] S. Brandenberger, O. Kröcher, A. Tissler, R. Althoff, Catal. Rev. 50 (2008) 492.
[2] C. Ciardelli, I. Nova, E. Tronconi, D. Chatterjee, B. Bandl-Konrad, Chem. Commun. (2004) 2718.
[3] A. Grossale, I. Nova, E. Tronconi, J. Catal. 265 (2009) 141.
[4] A. Grossale, I. Nova, E. Tronconi, Catal. Lett. 130 (2009) 525.
[5] A. Grossale, I. Nova, E. Tronconi, D. Chatterjee, M. Weibel, J. Catal. 256 (2008) 312.
[6] I. Nova, C. Ciardelli, E. Tronconi, D. Chatterjee, B. Bandl-Konrad, Catal. Today 114 (2006) 3.
[7] A. Savara, M.-J. Li, W.M.H. Sachtler, E. Weitz, Appl. Catal. B Environ. 81 (2008) 251.
[8] A. Savara, W.M.H. Sachtler, E. Weitz, Appl. Catal. B Environ. 90 (2009) 120.
[9] Y.H. Yeom, J. Henao, M.J. Li, W.M.H. Sachtler, E. Weitz, J. Catal. 231 (2005) 181.
[10] J.H. Kwak, J.H. Lee, S.D. Burton, A.S. Lipton, C.H.F. Peden, J. Szanyi, Angew. Chem. Int. Ed. 52 (2013) 9985.
[11] C. Paolucci, A.A. Verma, S.A. Bates, V.F. Kispersky, J.T. Miller, R. Gounder, W.N. Delgass, F.H. Ribeiro, W.F. Schneider, Angew. Chem. 126 (2014) 12022.
[12] M.P. Ruggeri, A. Grossale, I. Nova, E. Tronconi, H. Jirglova, Z. Sobalik, Catal. Today 184 (2012) 107.
[13] M.P. Ruggeri, I. Nova, E. Tronconi, Top. Catal. 56 (2013) 109.
[14] M. Iwasaki, K. Yamazaki, H. Shinjoh, Appl. Catal. A Gen. 366 (2009) 84.
[15] R.Q. Long, R.T. Yang, J. Catal. 207 (2002) 224.
[16] P.S. Metkar, M.P. Harold, V. Balakotaiah, Appl. Catal. B Environ. 111–112 (2012) 67.
[17] H. Sjövall, R.J. Blint, L. Olsson, Appl. Catal. B Environ. 92 (2009) 138.
[18] I. Ellmers, R.P. Vélez, U. Bentrup, A. Brückner, W. Grünert, J. Catal. 311 (2014) 199.
[19] D. Wang, L. Zhang, K. Kamasamudram, W.S. Epling, ACS Catal. 3 (2013) 871.
[20] M. Rivallan, G. Ricchiardi, S. Bordiga, A. Zecchina, J. Catal. 264 (2009) 104.
[21] M.P. Ruggeri, T. Selleri, M. Colombo, I. Nova, E. Tronconi, J. Catal. 311 (2014) 266.
[22] G. Delahay, D. Valade, A. Guzmán-Vargas, B. Coq, Appl. Catal. B Environ. 55 (2005) 149.
[23] Q. Sun, Z.-X. Gao, B. Wen, W.H. Sachtler, Catal. Lett. 78 (2002) 1.
[24] L. Lietti, M. Daturi, V. Blasin-Aubé, G. Ghiotti, F. Prinetto, P. Forzatti, ChemCatChem 4 (2012) 55.
[25] P.S. Metkar, V. Balakotaiah, M.P. Harold, Chem. Eng. Sci. 66 (2011) 5192.
[26] M. Colombo, I. Nova, E. Tronconi, Catal. Today 151 (2010) 223.
[27] M. Colombo, I. Nova, E. Tronconi, Appl. Catal. B Environ. 111–112 (2012) 433.
[28] A. Grossale, I. Nova, E. Tronconi, Catal. Today 136 (2008) 18.
[29] L. Castoldi, I. Nova, L. Lietti, P. Forzatti, Catal. Today 96 (2004) 43.
[30] S. Hodjati, P. Bernhardt, C. Petit, V. Pitchon, A. Kiennemann, Appl. Catal. B Environ. 19 (1998) 221.
[31] F. Prinetto, G. Ghiotti, I. Nova, L. Lietti, E. Tronconi, P. Forzatti, J. Phys. Chem. B 105 (2001) 12732.
[32] F. Prinetto, G. Ghiotti, I. Nova, L. Castoldi, L. Lietti, E. Tronconi, P. Forzatti, et al., Phys. Chem. Chem. Phys. 5 (2003) 4428.
[33] Y. Chi, S.S.C. Chuang, J. Phys. Chem. B 104 (2000) 4673.

[34] I.S. Pieta, M. García-Diéguez, C. Herrera, M.A. Larrubia, L.J. Alemany, J. Catal. 270 (2010) 256.
[35] I. Nova, L. Castoldi, L. Lietti, E. Tronconi, P. Forzatti, F. Prinetto, G. Ghiotti, J. Catal. 222 (2004) 377.
[36] L. Castoldi, L. Lietti, I. Nova, R. Matarrese, P. Forzatti, F. Vindigni, S. Morandi, F. Prinetto, G. Ghiotti, Chem. Eng. J. 161 (2010) 416.
[37] I. Malpartida, M.O. Guerrero-Pérez, M.C. Herrera, M.A. Larrubia, L.J. Alemany, Catal. Today 126 (2007) 162.
[38] A.A. Davydov, C.H. Rochester, Infrared Spectroscopy of Adsorbed Species on the Surface of Transition Metal Oxides, Wiley, Chichester, New York, 1990, p. 54.
[39] V. Matsouka, M. Konsolakis, R.M. Lambert, I.V. Yentekakis, Appl. Catal. B Environ. 84 (2008) 715.
[40] S. Brandenberger, O. Kröcher, A. Tissler, R. Althoff, Appl. Catal. B Environ. 95 (2010) 348.
[41] E.W. Kaiser, C.H. Wu, J. Phys. Chem. 81 (1977) 1701.